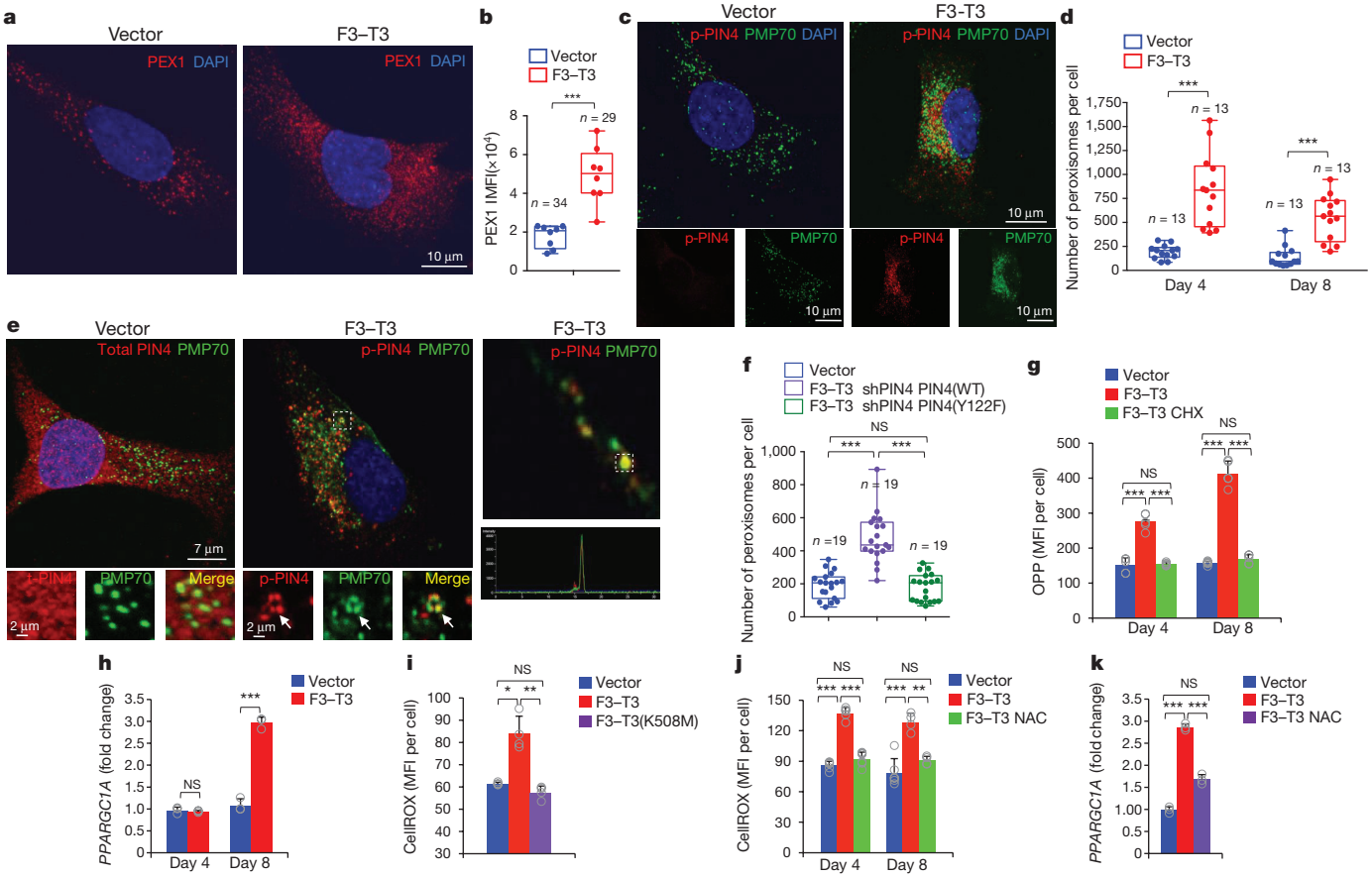

Figure 4 | Expression of F3–T3 fusion induces peroxisome biogenesis through phosphorylation of PIN4(Y122). a, Representative confocal micrographs of PEX1 immunostaining (red) and DAPI (blue) in vector and F3–T3-expressing human astrocytes. **b**, Quantification of PEX1 IMFI in samples stained as in **a** ($n = 34$ and 26 cells for vector and F3–T3, respectively). **c**, Representative confocal micrographs of double (top) and single (bottom) immunostaining for phospho-PIN4(Y122) (p-PIN4, red) and PMP70 (green) in vector and F3–T3-expressing human astrocytes. **d**, Quantification of peroxisome number per cell 4 and 8 days after F3–T3 expression in human astrocytes ($n = 13$ cells). **e**, Representative confocal micrographs of double immunostaining for total PIN4 (t-PIN4) and PMP70 in vector-expressing (left) or phospho-PIN4(Y122) and PMP70 in F3–T3-expressing (middle) human astrocytes. Arrowheads, phospho-PIN4(Y122)–PMP70 co-localization (bottom). Right, phospho-PIN4(Y122)–PMP70 co-localization (top) with corresponding spectral intensity profile (bottom); co-localization coefficients: Pearson's correlation $r = 0.935963$; Mander's overlap = 0.959905; Mander's overlap coefficients $k_1 = 0.934640$, $k_2 = 0.985853$; colocalization coefficients $c_1 = 1.000000$, $c_2 = 0.999792$. **f**, Quantification of peroxisome number per cell in F3–T3 human astrocytes following silencing of *PIN4* and expression of PIN4(WT) or PIN4(Y122F) ($n = 19$ cells). **g**, Quantification of protein biosynthesis by O-propargyl-puromycin (OPP) incorporation in human astrocytes that were treated as in **d**. Cycloheximide (CHX)-treated cultures are used as negative controls ($n = 5$ technical replicates). **h**, RT–qPCR of *PPARGC1A* in human astrocytes that were treated as in **d** ($n = 3$ technical replicates). **i**, Quantification of cellular ROS in vector-, F3–T3- and F3–T3-expressing human astrocytes. Bar graphs from one representative experiment ($n = 4$ technical replicates). **j**, Analysis of cellular ROS in human astrocytes that were treated as in **d**. Bar graphs from one representative experiment ($n = 5$ or 6 technical replicates). **k**, RT–qPCR of *PPARGC1A* in vector- or F3–T3-expressing cells that were treated with vehicle or *N*-acetyl-L-cysteine (NAC) ($n = 3$ technical replicates). Data are mean ± s.d. (**g**–**k**). *P*-values: **b**, **d**, **f**, two-sided MWW test; **g**–**k**, two-tailed *t*-test with unequal variance. Box plots span the first to third quartiles and whiskers indicate the smallest and largest values. Experiment in **i** was repeated twice; all other experiments were repeated three times with similar results.

Fig. 7q) and impaired *in vivo* tumour growth of F3–T3;shTrp53 mGSCs but not HRAS(12V)shTrp53 mGSCs (Extended Data Fig. 7r–v). Next, we developed a brain tumour model in *Drosophila* by ectopically expressing human F3–T3 using the glial-specific driver *repo-Gal4* (ref. 21). *repo-Gal4*–F3–T3 transgenic flies manifested glial neoplasia with enlargement and malformation of the larval brain lobe and ventral nerve cord, leading to larval lethality (Extended Data Fig. 8a, b). Cell number and proliferation of glial cells were enhanced in *repo-Gal4*–F3–T3 flies (Extended Data Fig. 8c, d). Cell-autonomous RNA interference (RNAi)-mediated knockdown of *spargel (srl,* the *Drosophila* orthologue of *PPARGC1A*)[22] in *repo-Gal4*–F3–T3 flies reduced glial tumour volume and decreased the number of $Repo^+$ glial cells, without affecting *repo-Gal4*-driven F3–T3 protein expression in F3–T3-expressing flies or normal brain development in wild-type animals without F3–T3 (Fig. 3j, k and Extended Data Figs 8e–g, 9a–d). *srl* knockdown did not rescue *Repo-Gal4*–F3–T3 animals to adult viability, confirming that suppressors of glial neoplasia in *Drosophila* are infrequent rescuers of organismic lethality[23] (Extended Data Fig. 9e). *srl* knockdown in a *Drosophila* model of glioma driven by constitutively active EGFR ($dEGFR^{\lambda}$) and PI3K ($Dp110^{CAAX}$) in the glial lineage[24] resulted in minor to no effects on tumour volume, thus highlighting the specific sensitivity of F3–T3 tumorigenesis to the perturbation of *srl* expression (Extended Data Fig. 9f, g). RNAi-mediated knockdown of the *Drosophila* oestrogen-related receptor (*ERR*) also reduced F3–T3 glial tumour volume (Extended Data Fig. 9h, i).

To determine the mechanism by which phospho-PIN4(Y122) mediates F3–T3 signalling, we studied the subcellular compartmentalization of PIN4 and phospho-PIN4(Y122) and sought to uncover the set of cellular proteins interacting with PIN4. Unphosphorylated PIN4 was diffusely localized in the cytoplasm and nuclear membrane whereas phospho-PIN4(Y122) was concentrated in larger cytoplasmic vesicle-like structures that co-localized with F3–T3 (Extended Data